

## Cutting characteristics of beard hair

S. M. Thozhur · A. D. Crocombe · P. A. Smith ·  
K. Cowley · M. Mullier

Received: 5 December 2005 / Accepted: 13 March 2006 / Published online: 4 January 2007  
© Springer Science+Business Media, LLC 2007

**Abstract** The cutting behaviour of beard hair has been investigated quantitatively and qualitatively. High speed cutting tests were conducted on beard hair samples using a purpose built cutting rig (provided by Gillette, UK) to determine the cutting forces. High speed digital video photography was used to record the cutting process. In parallel with these tests, low speed cutting tests were undertaken within a scanning electron microscope (SEM) to gain a better understanding of the cutting process. Results from the high speed cutting tests showed that the peak cutting stresses are influenced strongly by moisture (the cutting stress for ‘wet’ samples is reduced by about 30% as compared to dry samples) while the effects on the cutting stress of other variables (subject age, blade approach angle and sample ageing due to prolonged storage) appeared to be less noticeable. The angle of cut was affected by the distance of the initial contact point (between the hair and the blade) from the base of the hair with the line of cut shifting towards the hair axis with increasing distance from the base. Qualitative observations from video-recordings and still images taken during the cutting tests, conducted in-situ within the SEM as well

as the high speed cutting rig, showed four main cutting mechanisms of hair, which are documented in this paper. The distance from the initial contact point to the base of the hair and the moisture level were the parameters which controlled the mechanism of failure. Qualitative observations of the sort reported here are a necessary pre-cursor to the development of finite element models to simulate a cutting operation.

### Introduction

Cosmetics industries have devoted considerable effort towards improving the design of the razor blade. However, the attention paid towards understanding the mechanical properties of beard hair, especially in cutting, has been relatively modest and mainly confined to in-house work in major cosmetic and toiletry industries. For a good understanding of the beard hair-cutting process, there is a clear need to develop and integrate the characterisation of microstructure, material property and cutting mechanisms with suitable mechanical models. The first two of these areas have been addressed by the authors in an earlier publication [1]. The work reported here was aimed at achieving a better quantitative and qualitative understanding of the behaviour of beard hair in cutting.

Based on studies of the physiology and structure of scalp hair by several authors [2–7], it is known that the microstructure of hair broadly consists of three distinct zones, namely the cortex, the medulla and the cuticle, with the cortex constituting the bulk of the hair and contributing mainly to the tensile strength [8]. The

---

S. M. Thozhur · A. D. Crocombe (✉) ·  
P. A. Smith  
School of Engineering, University of Surrey, Guildford, UK  
e-mail: a.crocombe@surrey.ac.uk

K. Cowley · M. Mullier  
Gillette Management Inc., Reading, UK

S. M. Thozhur  
e-mail: tmsreeram@hotmail.com

P. A. Smith  
e-mail: p.smith@surrey.ac.uk

tensile stress–strain response of scalp hair has also been researched reasonably thoroughly and a two-phase model for the hair comprising of water impenetrable “microfibrils” embedded in a water penetrable “matrix” appears to be widely accepted in order to explain the behaviour in tension [9 (as referred to in 10), 11, 12]). Work by Deem and Rieger [13] on the cutting of beard hair suggested that the force to cut hair is reduced by about 65% due to moisture. However, no data was reported for the actual force values and the authors also did not report any results on the cutting stress. With regard to converting force values to stress values, it was found [1] that the cross-sectional profile of beard hair could vary from being nearly elliptical to almost tri-lobal and the authors also developed a novel method to characterise the cross-sectional area of elliptical cross-sections accurately. These improvements were considered in the work reported in this paper.

There are many variables which influence the cutting behaviour of beard hair. In the present work, attention was focussed on the effects of moisture, subject age, blade approach angle, proximity of the initial contact point from the base of the hair and sample ageing on the cutting force for beard hair. These data were obtained through cutting tests performed in a specially designed high speed cutting rig. The cutting mechanisms of beard hair were also studied using video-recording of the cutting tests conducted both in the scanning electron microscope (SEM) and the high speed cutting rig. An in-situ straining stage was used for the cutting tests undertaken in the SEM. Emphasis was placed only on identifying the trends of variation and thus a detailed statistical analysis was not carried out on any of the data.

## Experimental methods

### Samples

Samples of facial hair were obtained from three different caucasian males of ages 61 (subject A), 53 (subject B) and 39 (subject C). Tensile data have been presented for the hair samples from these subjects in previous work [1]. Samples used in this study were harvested only from the cheek site of the subjects and had been kept in storage, following harvesting, for nearly a year. Although the effect of facial site was not considered in the present study, the earlier study showed that the facial site did not have a significant effect on the tensile properties [1]. A separate batch of fresh samples (kept in storage for only a few hours

following harvesting) from the cheek of subject C was used along with the earlier set to study the effect of sample ageing on the cutting properties.

### Quantitative characterisation of the cutting forces during high speed tests

Cutting tests were performed on beard hair samples using a high speed cutting rig. The hair was inserted into a thin slit at the narrow end of a custom made hollow elastomeric base in the shape of a truncated cone. The hair filament was inserted so as to have a length of a few millimetres protruding out of the cone through the slit. The elastomeric cone was then held in a hollow metallic cup compressed by screwing to a pneumatically driven carriage. The blade was fastened to a stationary force beam so as to align the cutting edge to face the incoming hair filament as shown in Fig. 1. During the tests, the hair fixture was positioned in order to align the slit perpendicular to the cutting direction so as to minimise any tendency for slippage of the hair during the cut.

The force beam was bi-axial using strain gauges to enable the forces on the blade during the cut to be measured in two orthogonal directions, i.e. the cutting direction ( $F_{CD}$ ) which is parallel to the direction of movement of the hair-holding unit and the tip bending direction ( $F_{TBD}$ ) which is perpendicular to the cutting direction. The beam was initially designed to have a natural frequency of 1.8 kHz. This was sufficiently high so that the vibration of the beam had a minimum effect

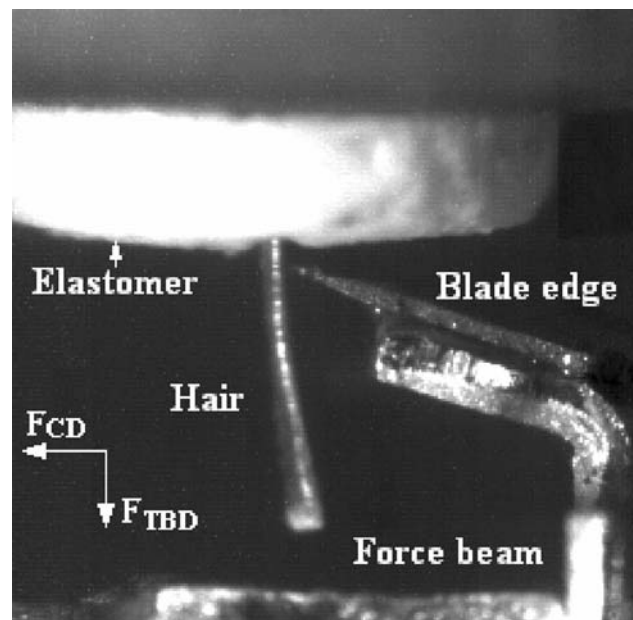


**Fig. 1** Test arrangement for a typical high speed cutting test

on the cutting response. Regular calibration of the beam was performed in-house and the conversion factors were used to evaluate the cutting forces. The calibration was done by suspending a standard weight from the force beam (holding the blade) using a thin metal wire of negligible mass. The output from the force beam (which appeared in volts) was monitored for different weights and a line of best fit was drawn for the data. The final calibration factor was then determined from the trend line. This procedure was followed for determining the calibration factors for both the orthogonal directions. The final conversion factors used were  $1V = 26.3\text{ g}$  ( $0.26\text{ N}$ ) for  $F_{\text{TBD}}$  and  $1V = 56.6\text{ g}$  ( $0.55\text{ N}$ ) for  $F_{\text{CD}}$ . Cutting tests were performed using beard hair in both wet and dry states. For wet tests, the samples were soaked in water for a period of 15 min prior to testing. In order to evaluate the cross-sectional area of dry test specimens, the cut hair was carefully removed from the elastomeric gripping cone (following a cutting test) and mounted on a card with the cut end overhanging the edge. Transverse measurements were made at a point close to the cut end at three different card orientations and the cross-sectional area was calculated using the method developed previously during tensile studies [1]. For evaluating the cross-sectional area of samples tested in the wet condition, the cut hair samples were allowed to dry following the test and the same method (adopted for the dry samples) was used along with a correction factor of 1.11 to account for swelling of the hair cross-section following wetting. This factor was based on trial observations made by the authors in an earlier study [1]. During the cutting tests, the distance from the base of the hair to the contact point with the blade was nominally set to  $150\text{ }\mu\text{m}$ . However, by analysing the results from the first series of cuts, it was seen that in some of the tests, the blade had cut through the elastomer base prior to making contact with the hair. Thus, it was decided to increase the contact distance from base to cutting point to  $200\text{ }\mu\text{m}$ . The cutting test schedules were planned based on the availability of the equipment and consequently there was a time gap of a few months between successive test schedules. The tests were carried out at  $0.3\text{ m s}^{-1}$ . This speed was chosen as being a reasonable approximation of a typical (manual) shave stroke. The angles of approach used for the blade from the cutting direction (horizontal in Fig. 1) were  $16^\circ$ ,  $22.5^\circ$  and  $28^\circ$ . While the  $22.5^\circ$  blades were used extensively for the cutting property characterisation tests, the  $16^\circ$  and  $28^\circ$  blades were variants introduced for studying the effect of the blade angle. Using an image capture facility associated with the high-speed cutting rig, still images of a selected set of samples were recorded immediately following the test to study the variation of the cut angle

as a function of the distance between the point of contact between the hair and the blade from the base of the hair.

## Qualitative characterisation of cutting process

### *Video-recording of SEM cutting tests*

In order to observe the mechanism of fracture of hair during the cutting process in more detail, cantilever cutting tests were performed on hair samples inside the SEM. A straining stage developed at the University of Surrey by Schoenewald (as described in [14]) for testing ceramic and polymeric materials in tension was modified to carry out cutting tests in the specimen chamber of the Hitachi S-4000 SEM. The straining stage was driven by a 12 V 1 Amp 2-phase DC stepper motor, a belt drive and a gear box. The set up enabled the fixture holding the hair to move towards the blade and speeds could be varied from  $0.01\text{ mm min}^{-1}$  up to  $0.4\text{ mm min}^{-1}$  by means of a Labview program running on an Apple Macintosh SE microcomputer with a National Instruments Lab-SE card which was interfaced to the straining stage. A photograph of the hair and blade holding fixtures that were attached to the straining stage for conducting the cutting tests is shown in Fig. 2.

The blade was bonded to the blade holding fixture so as to make an angle of  $22.5^\circ$  to the cutting direction. The hair, in turn, was bonded into an elastomeric cone identical to that used in a high speed cutting test. The base of the elastomeric cone was then bonded on to the hair holding fixture. The mounted hair was sputter coated with a thin layer of gold to prevent charging inside the SEM chamber. The fixtures were then mounted on the straining stage which was subsequently

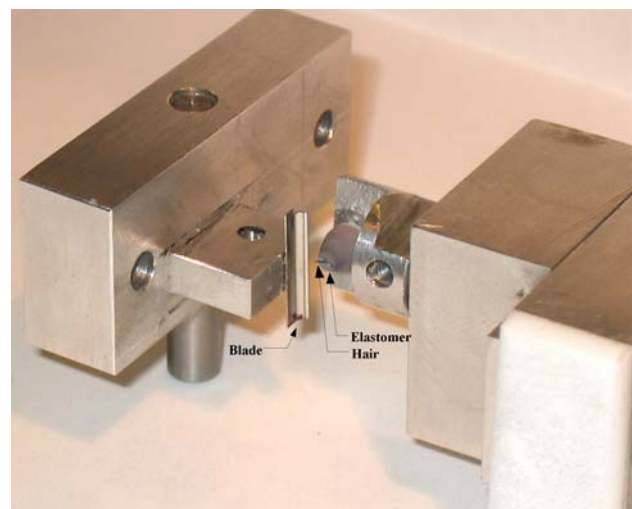


**Fig. 2** Hair and blade holding fixtures used for cutting tests in the SEM

attached to a platform within the specimen chamber of the SEM. The working distance used while recording the tests was 11 mm. The video recording was carried out using an image processing unit attached to the SEM electron detector using the software “Pixiescan” installed in a PC that logged the image data as received from the image capturing unit. The quality of the video depended on the scanning speed set in the SEM, which limited the “real time” recording capability. The scan speed was thus chosen to obtain the best compromise between the two requirements. On occasion, the test was interrupted in order to obtain better quality images. The video recordings from the cutting tests were complimented by conventional scanning electron microscopy of the cut hair samples.

The low speed tests were conducted primarily to identify clearly any possible mechanisms of failure in good detail. However, since the cutting speeds used in these tests were not comparable to real life shaving speeds, complementary cutting tests were conducted and video-recorded in the high speed cutting rig as mentioned in the next section with a view to observe and relate the cutting mechanisms with those observed in the low speed tests conducted in the SEM.

#### *Video-recording of high speed cutting tests*

Selected cutting tests performed in the high speed cutting rig were video-recorded using a high speed image capture facility associated with the rig. The video-recording was carried out at 50,000 frames per second.

### **Cutting force results**

#### Variation of cutting forces

A typical set of data from the high speed cutting tests is shown in Fig. 3. The curves show the oscillation of the blade following a cut. The peak values of the forces in the cutting (CD) and tip bending (TBD) directions were determined from the force response data. The force output was given initially in volts. This was converted into force using appropriate calibration factors which were different for the two directions. In most of the tests, every subsequent peak in the cutting and tip-bending direction force curves was lower than the previous peak as expected. However, the results from a few tests did not exhibit this response. A possible cause of this was the blade cutting into the elastomer prior to making contact with the hair. Although precautions were taken while

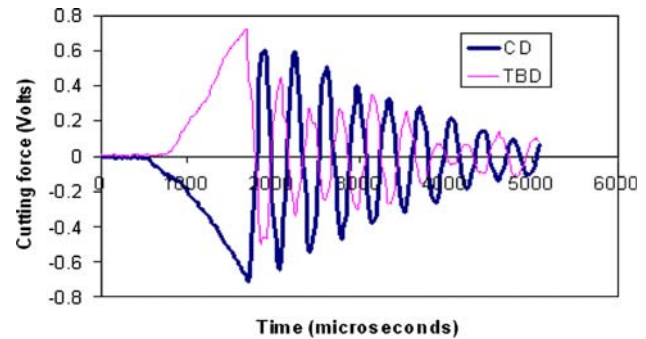


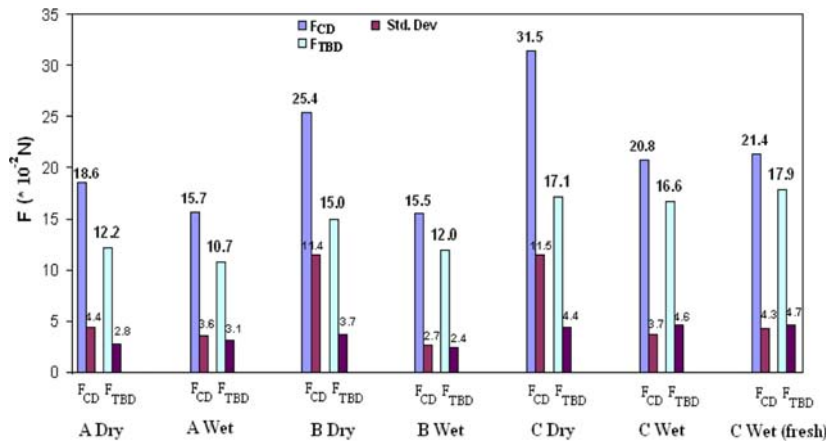
**Fig. 3** A typical response obtained from the force beam following a cutting test showing the blade oscillations after the cut (characterised by the initial peak values of the loads)

setting the initial contact point to avoid this problem (as indicated earlier), it is possible that in some of the subsequent tests, the problem still existed due to the high velocity of the hair holding fixture. Such test results were considered to be invalid and were not included. In excess of 180 cutting tests were performed in order to achieve a good understanding of the effect of different variables such as subject age, blade angle, moisture and ageing. About 150 tests were performed with 22.5° blades using 25 samples each for wet and dry tests from all the three subjects ‘A’, ‘B’ and ‘C’. About 10 freshly harvested samples taken from subject ‘C’ were used for studying the ageing effect on the cutting properties in the wet condition. About 20 cutting tests were conducted on freshly harvested samples using 16° and 28° blades using 10 samples each for the two blade angles.

Figure 4 shows the variation of the average cutting forces in the cutting and tip bending directions for the range of specimens tested using 22.5° blades. It appears from the data that the force in the cutting direction was higher than that in the tip-bending direction. In all the cases, moisture reduced the force in the cutting direction more than in the tip-bending direction. It needs to be pointed out that although the distance from the base to the cutting point was set to a fixed value of 200  $\mu\text{m}$  at the start of all tests, the movement of the hair holding fixture at high velocity caused the point of contact to change from this value in many cases. The actual value was determined by recording still images of the cut samples immediately following the test. It seems likely that a change in the point of contact will alter the cutting and tip bending direction forces. This would be one of the reasons for the variations between the tests. It also appears (from the data for subject C) that sample ageing did not affect the ‘wet’ cutting forces noticeably (see data for C Wet and C Wet (Fresh) in Fig. 4)



**Fig. 4** Variation of forces in cutting and tip bending directions for samples from all three subjects ‘A’, ‘B’ and ‘C’ cut using 22.5° blades for ‘wet’ and ‘dry’ conditions.



Variation of nominal cutting stress

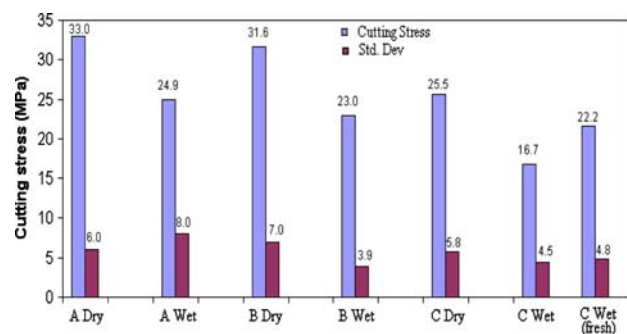
*Effect of subject, moisture and ageing*

Figure 5 shows the variation of the average nominal cutting stress over the sample set based on subject, moisture and sample ageing. The cutting stress was defined as the resultant force (*R*) divided by the hair cross-sectional area. The resultant force was calculated as the square root of the sum of the squares of the components along the cutting and tip-bending directions. i.e.,

$$R = \text{SQRT} [(F_{CD})^2 + (F_{TBD})^2]$$

As indicated earlier, a number of test results had to be omitted since some tests were invalid.

It can be seen that the data for the different sample sets are quite consistent, with low standard deviations in most cases. Moisture reduced the cutting stress through a combination of a reduction in the cutting force and an increase in the cross-sectional area of hair due to swelling. For subjects ‘A’ and ‘B’, the cutting stress values are quite similar for the wet (24.9 MPa, 23 MPa) and dry (33 MPa, 31.6 MPa) states consid-



**Fig. 5** Variation of average cutting stress over the entire sample set cut using 22.5° blades

ered separately. This was not the case for the forces which clearly shows that accounting for the cross-sectional area was vital. While subject B gave a marginally higher cutting force than subject A, the larger cross-sectional area of subject B hair (reported in [1]) made the cutting stress consistent with that of subject A. It can also be seen that the data from subject ‘C’ show slightly lower wet and dry cutting stresses than the rest of the sample set. This is not unexpected because the percentage increase between the average resultant cutting force of subject C and that of subjects ‘A’ and ‘B’ was far less than the corresponding increase in the average cross-sectional areas (reported in [1]). Also, it can be seen that the fresh samples from subject ‘C’ show a marginally higher average cutting stress than the aged samples. This is because while the resultant cutting forces of the fresh and aged samples were quite similar, the average cross-sectional area of the fresh samples was slightly smaller than that of the aged samples as shown in Fig. 6. This implies that

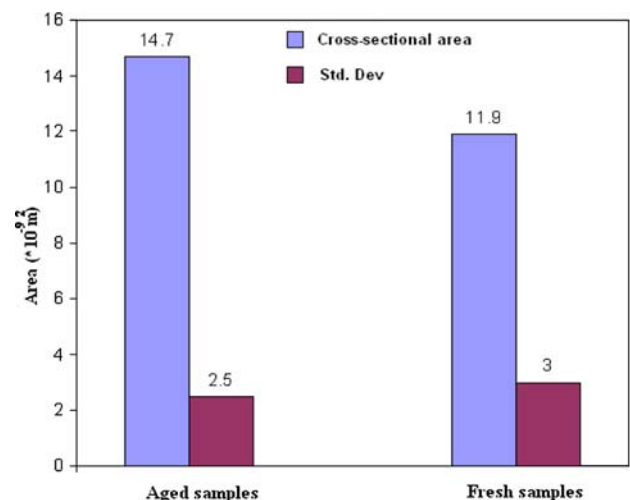


**Fig. 6** Average cross-sectional areas of samples from subject ‘C’ (aged and fresh) used for the cutting tests with 22.5° blades

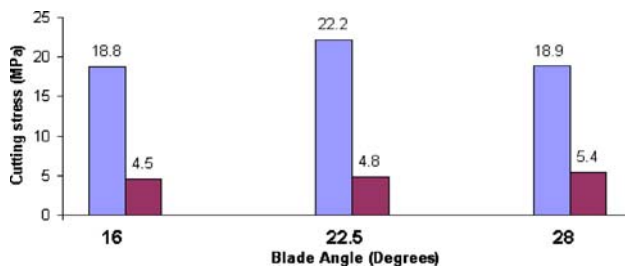


**Fig. 7** Variation of average cutting stress in freshly harvested samples from subject 'C' across different blade angles

there could be some ageing affect on the cutting properties.

#### *Effect of blade angle*

Figure 7 shows the variation of the average cutting stress in fresh samples from subject 'C' across different blade angles. The results seem to suggest that changing the blade angle (within the selected range) does not affect the nominal cutting stress. The same effect would be observed on the corresponding cutting forces as well since the samples came from the same subject and were harvested at the same time thus making the cross-sectional areas more or less similar over the entire set.

#### Variation of cut angle with distance from base

As noted earlier, despite fixing the distance from base to the intended contact point prior to a cutting test, the movement of the hair holding fixture at high velocity caused the position of the initial contact point to vary between the tests. Although this was undesirable, it facilitated a study of variation of the angle of cut as a function of the distance of the contact point of hair and blade from the base of the hair. Figure 8 shows a typical set of 'after-cut' images taken in the cutting rig

for samples from subject 'C' cut 'wet' using 22.5° blades. Figure 8a shows a sample cut at about one and a half hair diameters away from the base, (b) shows a sample cut at about three hair diameters away from the base while (c) shows a sample cut at about six hair diameters away from the base. Taking the hair axis as a reference, the angle of cut was measured as a function of distance from the base (measured in hair diameters) and the results for a selected set of samples from the three different subjects tested both 'wet' and 'dry' are shown in Fig. 9. Figure 10 shows a schematic of a fractured hair filament to illustrate how the angle of cut was determined. It can be seen that in most cases, the cut angle decreased slightly with increasing distance from base although the trend was a little weak in some data-sets. This observation is important, since it implies that as the contact point between the blade and the hair moved further away from the base, the line of the cut was likely to be oriented more along the hair axis. This is consistent with the observations of the cutting mechanisms outlined below.

#### **Observation of cutting mechanisms**

Observations from video-recordings of cutting tests in the SEM

Cutting tests were performed on samples taken from the cheek of subject 'C' using a straining stage within the SEM and the tests were video-recorded as discussed earlier. Since the SEM operates under conditions of high vacuum, the tests were undertaken on dry samples only. About 35 cutting tests were performed in the present work of which about 15 provided clear details of the cutting process. Twenty or so tests were unsuccessful, owing to factors such as the blade cutting into the elastomeric base, the blade or the hair becoming



**Fig. 8** Still video images of hair samples (a) cut at about one and a half hair diameters away from the base, (b) cut at about three hair diameters away from the base and (c) cut at about six hair diameters away from the base

**Fig. 9** Variation of angle of cut with distance from base normalised by the hair diameter

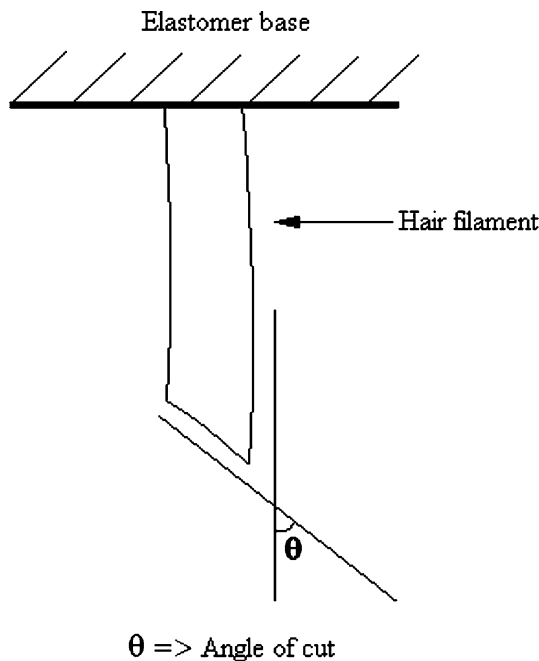
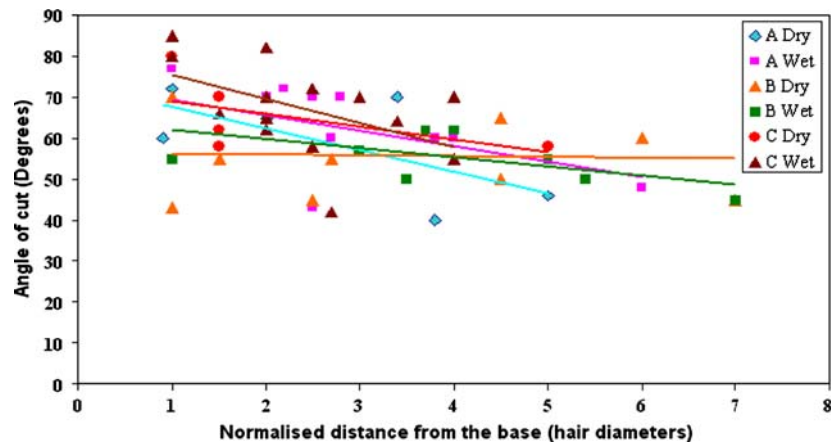


**Fig. 10** Schematic illustrating the measurement of the angle of cut

detached from the holder (as a result of poor bonding) and the fixing adhesive covering the hair. In addition, there were unexpected complications during the recording process such as the quality of the video recording being poor as a result of unexpected vibrations of the straining stage during the test and blocking of the field of view of the cutting process by the blade edge.

The tests that were successful gave very useful insights into the behaviour of hair during cutting. The cutting mechanisms were mainly influenced by the initial point of contact. Table 1 shows a summary of the mechanisms observed. Images showing details of these mechanisms are included in Figs. 11–17. Whilst some of the figures were captured during the cutting process, others were obtained whilst stationary, either

during the cutting process or during a separate examination of the fracture surface of the cut sample. As an indication of the scale in Figs. 11–17, an estimate of the effective hair diameter is 140  $\mu\text{m}$  over the entire range of samples. The four mechanisms of failure (Table 1) observed in the cutting tests conducted in the SEM are outlined below.

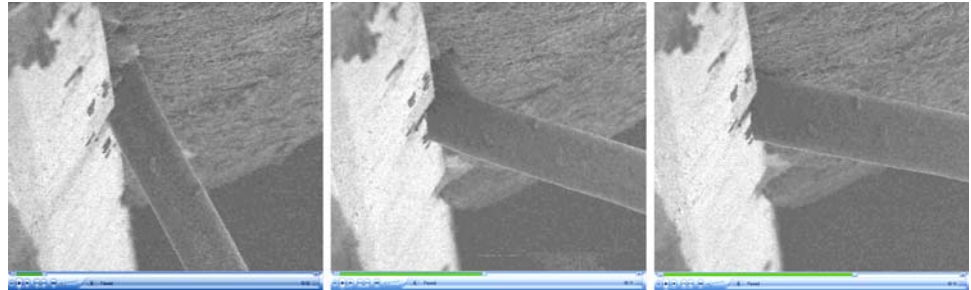
*Mechanism 1 (M1):* For cuts close to the base of the hair (less than two hair diameters away from the base), it is likely that following a partial cut, the crack induced radially will travel along the hair axis towards the base. This is possible if the base is quite stiff or when the major axis of the hair is lying along the direction of the blade travel thus offering a high resistance to bending (since the second moment of the area of the elliptical hair in that orientation is high). If this happens a longitudinal ‘split’ is created (see Figs. 11 and 12) which separates a small portion of the hair (running axially from the base to the contact point and radially from the surface up to the core) from the rest of the filament. Following the longitudinal split, the blade proceeds to cut the remaining portion of the hair lying ahead of it normal to the hair axis. This type of behaviour is categorised as Mechanism 1 of failure. The longitudinal split is likely to be brought about by the high shear stresses existing between the cortical cells as a result of the forces on the hair.

*Mechanism 2 (M2):* Mechanism 2 is characterised by partial stable penetration of the blade into the hair followed by bending of hair and rapid fracture (see Figs. 13 and 14). This mechanism of failure is likely to occur when the point of contact between the blade and the hair is quite close to the base of the hair as in case of Mechanism 1. However, it is not clear as to what factors support the occurrence of M2 as against M1.

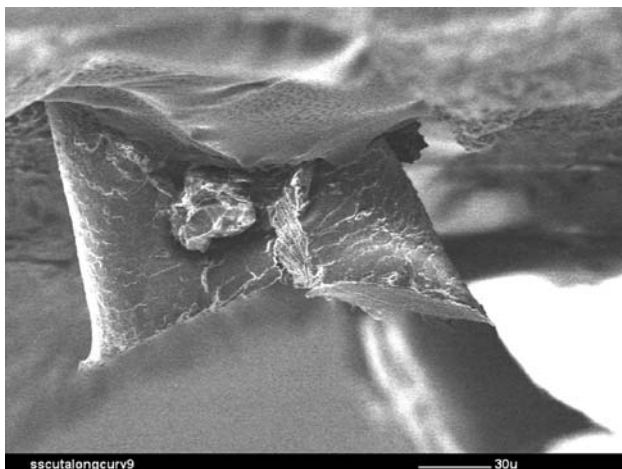
*Mechanism 3 (M3):* As the distance from the base to the point of contact between the blade and the hair increases beyond about three hair diameters, the hair

**Table 1** Mechanisms of failure observed in the SEM cutting tests

Mechanism notation	Mechanism of failure	Approximate distance of contact point from base	Reference figures
M1	Partial penetration and bending followed by longitudinal splitting of hair towards the base	<2 hair diameters	10, 11
M2	Partial stable penetration followed by bending of hair and rapid fracture	<2 hair diameters	12, 13
M3	Slipping of the blade on the hair surface, followed by partial penetration and then skiving leading to gradual fracture	4–6 hair diameters	14, 15
M4	Partial penetration followed by extreme skiving leading to propagation of blade along the hair length	>6 hair diameters	16

**Fig. 11** Series of video images from an SEM cutting test exhibiting failure mechanism M1

becomes more compliant and bends relatively easily. This makes the penetration of the blade normal to the hair axis less likely and causes the blade to slide over the hair surface until the cutting forces are high enough to cause penetration normal to the hair axis (see Figs. 15 and 16). Due to bending of the hair, the cut is inclined and thus the blade makes a ‘skiving’ cut at an angle across the hair rather than a normal cut. This characterises Mechanism 3 of failure which is likely to occur when the point of contact between the hair and the blade is between four to six hair diameters.

**Fig. 12** SEM image of the fractured end of the sample used for the cutting test depicted in Fig. 10 showing the longitudinal split

*Mechanism 4 (M4):* As the distance from the base to cutting point increases further, there is a more developed form of Mechanism 3 due to easy bending of the hair along the direction of blade propagation. This prevents the blade from cutting the hair perpendicular to the axis. Upon reaching the critical force value needed for penetration normal to the hair axis, the blade follows an inclined path cutting through the cuticles and part of the cortex until the medulla region is reached. Since the cut is inclined, there is a partial axial separation of the hair from the point of contact going towards the free end (somewhat analogous to Mechanism 1). This causes extreme bending of the remnant ‘uncut’ cross-section lying ahead of the blade (since the partial axial split drastically reduces the second moment of area and thus the resistance offered by the hair to the cut) and so the blade path becomes nearly parallel with the axis of the hair making use of the low resistance path provided by the medulla to the blade. The blade thus cuts the hair axially thereby splitting the shaft longitudinally into two (see Fig. 17). This kind of failure is categorized as Mechanism 4 and is likely to occur when the distance from the base of the hair to the point of contact between the blade and the hair is more than six hair diameters.

Observations from video-recordings of cutting tests in high speed cutting rig

Additional high speed cutting tests were video-recorded using a high speed recording facility. The



**Fig. 13** Series of video images from an SEM cutting test exhibiting failure mechanism M2

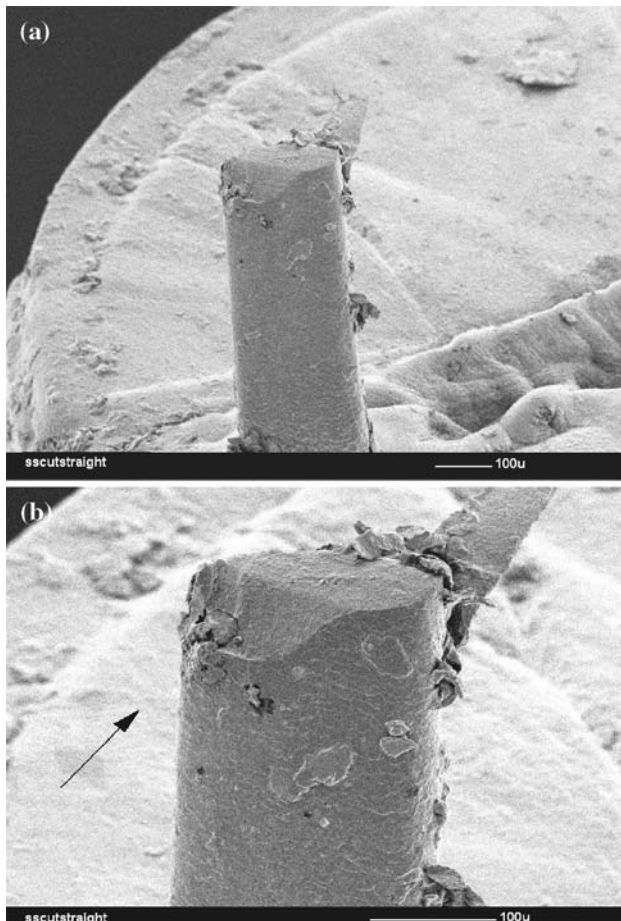
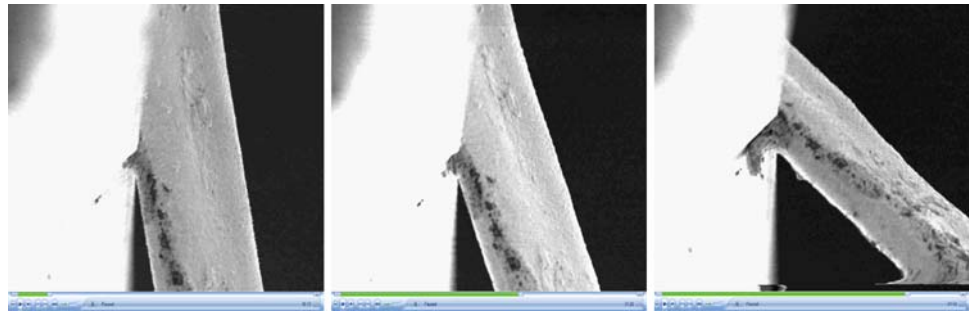


**Fig. 14** SEM images of the fractured end of the sample used for the cutting test depicted in Fig. 12. The arrow shows the direction of the cut

tests were performed on fresh beard hair samples harvested from Subject ‘C’ since the cutting tests performed in the straining stage were carried out on aged samples from the same subject. Thus, in order to assess the effect on the cutting mechanisms of both (a) cutting speed and (b) ageing of samples, it was decided to record the high speed tests on fresh samples. However, a few cutting tests on ‘wet’ samples were also recorded in order to check for any new mecha-

nisms of failure that were not identified in the SEM cutting tests, which could be undertaken on dry samples only. Just over 15 tests each in wet and dry conditions were carried out. However, some of these were not successful and a total of about 10 wet tests and 7 dry tests were performed and recorded successfully. Table 2 categorises the mechanisms observed in the high speed cutting tests in both wet and dry conditions for a selected set of samples using the same notation as adopted in Table 1. Figures 18 and 19 show stills of a few samples cut ‘dry’ and ‘wet’ respectively taken immediately following the cutting test using the same video capture unit that was used to record the cutting test itself. The nominal distance from the base to the cutting point was preset to 200  $\mu\text{m}$ . The results show that if the contact point is close to the base, then mechanism 1 dominates the dry tests while mechanism 2 dominates the wet tests. The reason for this is unclear, but it could be that moisture reduces the shear stresses between the cortical cells thereby preventing a longitudinal split.

## Discussion

Cutting force measurements from the high speed cutting tests showed that the effect of moisture on the cutting direction force was greater (bringing the value down by a factor of about 1.4) than on the tip-bending direction force (bringing the value down by a factor of about 1.14) as shown in Fig. 4. This is not unexpected since the cutting direction force is mainly governed by the resistance offered by the matrix phase to the advancing blade. The cutting direction force value drops due to hydration since the matrix gets plasticised and the resistance to the cut is offered mainly by the alpha helices lying ahead of the advancing blade. The tip bending direction force, on the other hand, would be governed by the extension of the alpha helical microfibrils (which are water impenetrable) as the hair bends and pulls the blade edge. Also, the effect of sample ageing on the cutting forces

**Fig. 15** Series of video images from an SEM cutting test exhibiting failure mechanism M3

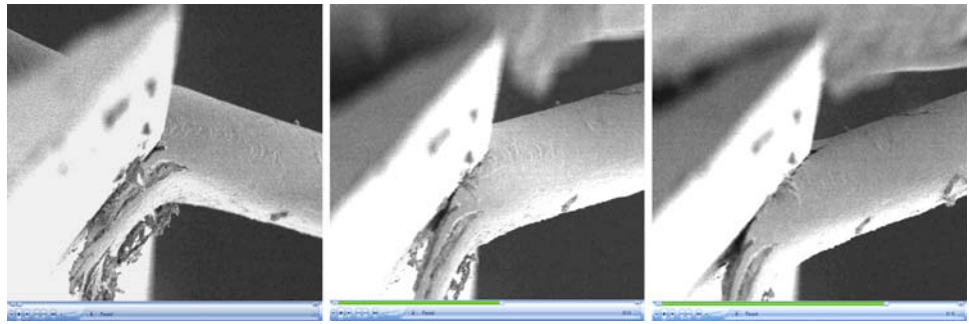


**Fig. 16** Still images taken in the SEM part way during the test depicted in Fig. 15 (a) showing the cuticles and part of the cortex from one side of the partially cut hair lying over the visible edge of the blade and (b) showing a segment of the hair over which the blade slid prior to commencement of normal penetration

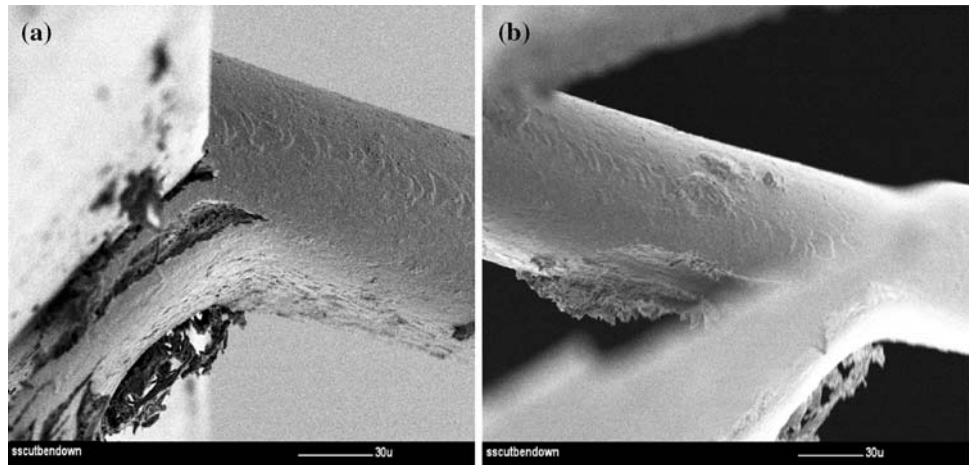


**Fig. 17** Series of video images from an SEM cutting test exhibiting failure mechanism M4



**Table 2** Mechanisms of failure observed in the high speed cutting tests

Mechanism	Percentage observed in 'Dry' tests	Percentage observed in 'Wet' tests
M1	40	15
M2	20	85
M3	–	–
M4	40	–

for 'wet' samples was found to be minimal as seen in Fig. 4. While softening of the matrix phase due to hydration would explain the cutting direction forces being similar in spite of ageing, the replenishment of the hydrogen bonds stabilising the alpha helices

(possibly lost due to ageing) by hydration could be the reason for the tip bending direction forces being similar.

A study of the effect of ageing on samples from Subject C showed that the average cross-sectional area of the aged samples was slightly larger than that of the fresh samples as shown in Fig. 6. This may be an effect of the point to point variation in area within a sample. As mentioned earlier, the area was calculated for every sample at only one point in close vicinity to the cutting zone. Another factor that might contribute to the difference in cross-sectional area could be biological changes experienced by the subject over the period between initial and subsequent harvesting. Given that

**Fig. 18** Still after-cut images of two samples cut ‘dry’ in high speed rig. Notice the hair cross-section getting drastically thinner towards the free end showing evidence of failure mechanism M4 in both samples

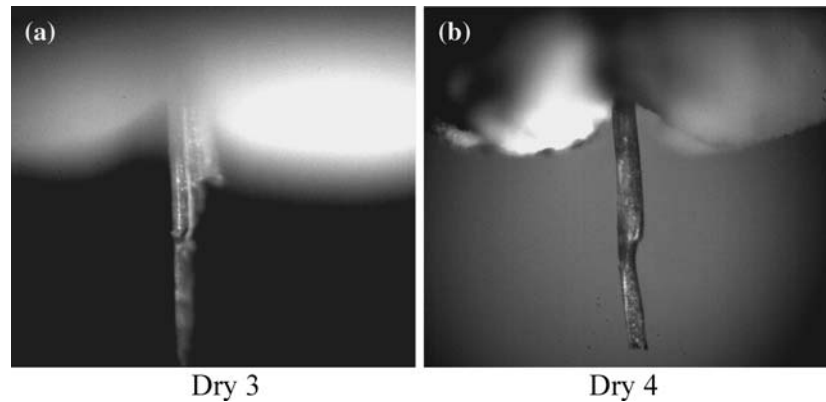
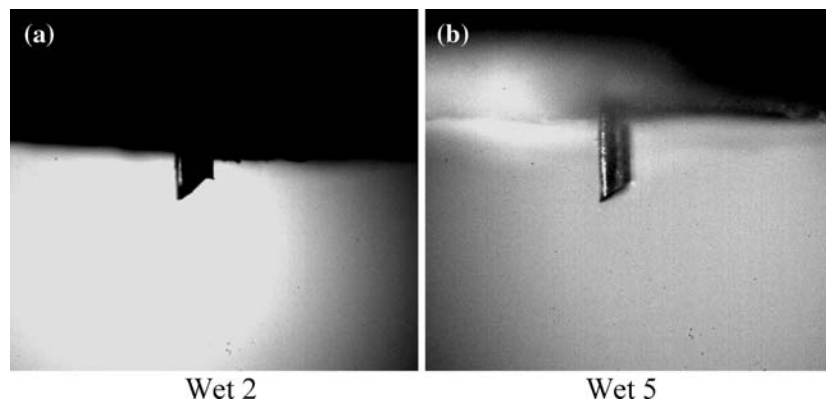


**Fig. 19** Still after-cut images of samples cut ‘wet’ in high speed rig. The samples clearly show evidence of failure mechanism M2



the fresh samples were harvested from the subject nearly a year after the old set, any biological changes in the subject could possibly have affected the hair and its cross-sectional area.

It was found that varying the blade angle (within the selected range) did not influence the nominal ‘wet’ cutting stress noticeably (Fig. 7). Considering the well established two-phase model used for explaining the behaviour of scalp hair in tension ([9 (as referred to in 10), 11, 12]) a possible explanation for this observation would be that since the samples were cut ‘wet’, the contribution from the water-penetrable matrix and thus the cutting direction force would be minimal. Changing the blade angle is likely to affect only the normal penetration of the blade and thus the cutting direction force. However, as discussed earlier, the presence of moisture reduces the cutting direction force and thus the effect of changing blade angle on the cutting direction force is not very noticeable. The tip-bending direction force, on the other hand, is unlikely to be affected much by changing the blade angle (within the selected range) as compared to the cutting direction force since the tip-bending direction force is associated with the bending of the hair and the friction between the hair and the blade. However, the magnitude of the change in the tip-bending direction force

with changing blade angle could vary when the wet and dry results are compared. Since the contribution of the matrix to the resistance offered by the hair is reduced by water, the main contribution to the resultant cutting force would have to come from the water impenetrable ‘microfibrils’. Thus, the overall resultant cutting force and consequently the cutting stress would be more or less similar for different blade angles.

The observations from the video-recording of cutting tests conducted in the SEM showed that the mechanisms of failure M1 and M2 exhibited a common feature during the failure process which was the rapid commencement of the cut perpendicular to the hair axis. This happens because, for cuts close to the base, it is difficult for the blade to slide over the hair (especially if the curvature of the hair opposes the blade travel) or for the hair to resist the cut perpendicular to the axis by bending and conforming to the blade motion. Thus the cut (perpendicular to the hair axis) commences quickly and proceeds in the same direction fairly easily in both M1 and M2. Mechanisms M3 and M4 were distinguished only by the extent of sliding of the blade over the hair and the extent of alignment of the direction of the cut towards the hair axis, both of which were higher in mechanism M4. Mechanism M3 (or M4) is also likely to occur when the

initial contact point is closer to the base if the supporting base is extremely compliant (which will facilitate easy bending of hair and prevent easy normal penetration of the blade into the hair) or if the quality of the blade edge is poor (which will also prevent easy normal penetration of the blade into the hair and thus cause the blade to slide over the hair surface).

The mechanisms observed in the high speed tests were consistent with those observed in the SEM cutting tests under similar conditions. However, much more detail was available in these latter tests. It can be suggested that sample ageing and cutting speed do not affect the main mechanisms of failure of beard hair in cutting. It needs to be pointed out there are other uncontrollable factors that might cause deviation of the behaviour of the cut from the expected mechanisms. Such factors may include quality of the blade edge, cross-sectional profile of the sample, and any possible damage induced in the hair filament prior to the test. For example, it can be observed from the Figs. 18 and 19 that the appearance of the elastomeric base is not consistent and this will lead to variations in the cutting pattern. Whilst every possible effort was made to ensure uniformity of the testing conditions, factors such as the nature of the hair fixture (which had to be screw fastened to the holder) and the high intensity lights (used while recording the cutting tests in the high speed cutting rig) targeted at the hair-blade interaction zone might have caused minor differences in the elastomer (due to elevated temperatures) which are seen in the after cut images. Nevertheless, considering the reasonable consistency between the observations made in the straining stage and high speed video recordings, it is suggested that the proposed mechanisms give a good representation of the cutting processes.

### Concluding remarks

The cutting forces and cutting mechanisms of beard hair have been studied. High speed cutting tests on real beard hair samples taken from the cheek of three different subjects gave an insight into the influence of variables such as subject age, moisture and sample ageing on the cutting properties. Moisture was the main variable that affected the peak cutting stress. In the presence of moisture, the peak cutting stress was brought down by almost 30%. Blade angle did not affect the cutting stress noticeably while the effect of ageing appears to be more

statistical than real due to the observed differences in the average areas of the two sample sets, despite coming from the same subject. Variation between the subjects could not be distinguished from the test scatter. From the cutting force data, it was found that moisture reduced the force in the cutting direction more than in the tip-bending direction. It was also found that the data for cutting stresses showed lesser scatter than the corresponding cutting force data. This was clearly influenced by the effective cross-sectional area characterisation method [1] used in the study.

The video recordings of SEM cutting tests and high speed cutting tests provided useful information regarding the possible mechanisms of failure of hair in cutting dependent on moisture and the initial contact point. Based on the observations, the mechanisms of failure of hair in cutting were classified into four categories. Mechanism M1 was characterised by a longitudinal splitting of the hair filament following a partial penetration of the blade into the hair and occurred in ‘dry’ cuts when the contact point between the hair and the blade is less than two hair diameters away from the base. Mechanism M2, which also occurred when the contact point was close to the base, was characterised by a partial stable penetration of the blade into the hair followed by a quick unstable cut and was more likely to occur in case of ‘wet’ cuts. Mechanism M3 mainly occurred when the contact point between the blade and the hair was about four to six hair diameters away from the base and was characterised by minor sliding of the blade over the hair surface followed by a skiving cut brought about by the bending of the hair. Mechanism M4 was an extreme case of M3 and occurred when the distance from the base to the contact point was more than six hair diameters and was characterised by extreme sliding of the blade over the hair surface followed by a partial skiving cut which ultimately travelled along the hair axis thereby cutting the hair shaft into two.

It is envisaged that the observations made in this study, combined with the earlier work on the structural characteristics and mechanical behaviour of beard hair [1] will inform finite element modelling of the cutting process. This will ultimately lead to a better understanding of the hair-cutting process.

**Acknowledgements** The authors would like to acknowledge the sponsorship offered by The Gillette Company to facilitate the research work discussed in this paper and the co-operation extended by the organisation through granting access to the high-speed cutting rig/video-recording apparatus.



**References**

1. Thozhur SM, Crocombe AD, Smith PA, Mullier M, Cowley K (2006) *J Mat Sci* 41(4):1109
2. Dawber RPR (1986) *Bioeng Skin* 2:1
3. Dawber R (1996) *Clin Dermatol* 14:105
4. Jones LN (2001) *Clin Dermatol* 19:95
5. Swift JA (1991) *Intl J Cosmet Sci* 13:143
6. Swift JA (1997) *AIM J EXS* 78:149
7. Watanabe H, Yahagi K. (1992) *Jpn J Tribol* 37(4):427
8. Feughelman M (1997) *Cosmet Sci Technol Ser* 17:1
9. Feughelman M (1982) *J Soc Cosmet Chem* 33:385
10. Sakai M, Nagase S, Okada T, Satoh N, Tsujii K (2000) *Bull Chem Soc Jpn* 73:2169
11. Feughelman M (1964) *Textile Res J* 34:539
12. Feughelman M (1994) *Textile Res J* 64(4):236
13. Deem D, Rieger MM (1976) *J Soc Cosmet Chem* 27:579
14. Trusty PA (1994) PhD thesis (University of Surrey)